Geophys J. R. astr. Soc. (1971) **25,** 511–538

Elasticity and Equations of State of Olivines in the Mg_2SiO_4-Fe_2SiO_4 System

D. H. Chung

(Received June 10 1971)

Summary

Presented first in this paper are the elasticity data of seven olivines as a function of pressure, temperature, and Fe/Mg ratio. The elasticity data include (i) P and S wave velocities and their first derivatives with respect to pressure and temperature, (ii) the shear and bulk moduli and their first pressure and temperature derivatives, and (iii) Poisson's ratio and its pressure and temperature derivatives (all evaluated at zero pressure and at ambient temperature). The critical thermal gradients for density and for P and S wave velocities are presented for olivine with different Fe/Mg ratios. Also presented are the Debye temperature and Gruneisen's parameters γ_G and δ_s for olivine as a function of Fe/Mg ratio. Next, incorporating these elasticity data with theories, equations-of-state parameters of olivine and olivine-transformed spinel as a function of Fe/Mg are found. The equations of state of olivine are then presented; a pressure-volume-temperature (PVT) relation for olivine is examined as a function of temperature and Fe/Mg ratio. Finally, based on F. Press's recent Monte Carlo solutions, the present elasticity data are related to the Earth's upper mantle within the framework of a peridotitic model. Typically, for 100 Fo, 50 Fo, and 100 Fa olivines, values of density ρ_0 (in g cm^{-3}), the P and S wave velocities (in km s^{-1}), the adiabatic bulk modulus K_s (in mb) and its pressure derivative dK_s/dp, Gruneisen's parameters γ_G and δ_s, the Debye temperature θ_D (in °K), and the critical thermal gradients G_i, where i stands for density and P and S wave velocities, are as follows:

Fe/Mg ratio	Phase	ρ_0	V_p	V_s	K_s	$\frac{dK_s}{dp}$	γ_G	δ_s	G_p	G_s	G_ρ	θ_D
0/10	01	3·217	8·534	4·977	1·281	5·04	1·21	4·0	24	12	31	753
	Sp	3·556	9·66	5·54	1·86	4·4	—	—	—	—	—	869
5/5	01	3·800	7·534	4·213	1·256	5·44	1·10	4·4	24	8	33	633
	Sp	4·209	8·85	4·92	1·93	4·8	—	—	—	—	—	765
10/0	01	4·393	6·637	3·494	1·220	5·92	1·02	4·7	23	2	35	523
	Sp	4·849	8·05	4·28	1·96	5·1	—	—	—	—	—	662

1. Introduction

A realization of the constitution of the Earth's interior is limited by our knowledge of the properties and the behaviour of various materials at high pressure and high temperature. This paper presents the elastic parameters of olivine measured as a function of pressure, temperature, and composition, and discusses equations of state of olivine as a function of varying the iron/magnesium ratio in the olivine lattice. Olivine, $(Mg_xFe_{1-x})_2SiO_4$, is an important rockforming mineral believed to be abundant in the Earth's upper mantle. Determination of the equations of state for olivine is therefore of particular interest to the study of the physical state and the chemical composition of this region of the Earth's interior. This paper studies some of the more important geophysical and thermodynamic properties associated with the effects of iron in olivine. The present report is a continuation of an earlier paper by this author on the elasticity of olivine in the forsterite-fayalite series at ambient conditions (see Chung 1970; referred to below as C1); it includes the elasticity data obtained under various pressure and temperature conditions.

There is abundant literature concerned with the elasticity of olivine. An extensive survey of the literature was made in the earlier report (see C1, p. 7357). A systematic comparison and discussion of these elasticity data at ambient conditions was also presented, and this will not be repeated in the present paper.

The first section of this paper presents a brief description of experimental procedure and olivine samples used, followed by the elasticity data of olivine as a function of pressure, temperature, and compositions. In the second part, equations of state for various olivines with different iron/magnesium ratios are given. A discussion is presented of the present olivine data and their relation to the Earth's mantle.

2. Olivine samples

The olivine samples used in this study were the same as those of the previous work by this author. They were produced by a pressure-sintering method. Along with the two end-member olivines, five other olivines with the following compositions were studied: 95 per cent Fo, 90 per cent Fo, 85 per cent Fo, 80 per cent Fo, and 50 per cent Fo, where " per cent Fo " designates a mole percent forsterite. The emphasis on these olivine compositions in this study was instigated by the present state-of-the-art hypothesis on the chemical composition of the Earth's upper mantle. The earlier paper discussed the chemical purities and character of these olivine samples (see C1, p. 7354), and readers are referred to the description found in that report.

3. Experimental method and procedure

The measurement of sound velocities at room conditions (at 23 °C and 1 bar), as a function of hydrostatic pressure to about 7·5 kb, and also a function of temperature, were made with the pulse-echo-overlap method. We used a simple piston-cylinder set-up of standard design (see Brace, Scholz & La Mori 1969, for example) as our pressure system. The pressure medium was reagent grade petroleum ether, and the pressure was read directly from a precalibrated 7500-bars Heise gauge. The readability of this gauge was better than 0·2 per cent of the pressure reading. X-cut and AC-cut quartz transducers with resonance frequencies of 10 to 20 MHz were used for generating compressional (P) and shear (S) waves respectively. The following materials for acoustic bonding between specimen and transducer were used: in the ultrasonic-pressure experiments, a 50 per cent mixture (by volume) of phthalic anhydride and glycerine; in the ultrasonic-temperature experiments, Nonaq stopcock

grease (Fisher Chemical Company) for low temperature measurements, and an epoxyphenolic resin (Bloomingdale Rubber Company) for high temperature measurements.

The following data were determined in our ultrasonic experiments: (a) both P and S velocities in each specimen at room conditions, (b) pulse repetition frequencies (PRF) corresponding to these velocities as a function of pressure to about 7·5 kb at 23 °C, and (d) these PRFs corresponding to the velocities at 1 bar in the temperature range of 0 to 200 °C.

The quantity of interest in the ultrasonic experiments, in which pressure is a variable, is the first derivative of an isotropic elastic modulus M_j with respect to hydrostatic pressure evaluated at zero-pressure; this will be denoted hereafter as $\{dM_j/dp\}_{p=0}$. This is an isothermal derivative, although the velocity-of-sound measurements involve an adiabatic process. Thus, the acoustic data resulting from such experiments are *thermodynamically mixed* isothermal pressure derivatives of the adiabatic modulus. For a modulus M_j, where the subscript $_j$ refers to either compressional (P) or shear (S) mode, we have

$$\left\{\frac{dM_j}{dp}\right\}_{p=0} = \left\{\frac{M_j}{3K_T}\right\}_{p=0} + \{M_j R_j\}_{p=o} \tag{1}$$

where $R_j = d(f_{jp}/f_{j0})^2/dp$, and this is obtained by fitting $(f_{jp}/f_0)^2$ versus pressure data to a straight line by the method of least squares, following Bacon (1953). K_T is the isothermal bulk modulus, and it is related to the adiabatic bulk modulus K_s by $K_T = K_s/(1+\alpha_v T\gamma_G)$, where α_v is the coefficient of volume expansion, γ_G is Gruneisen's ratio, and T is temperature in °K. It is clear from equation (1) that the measurements of isotropic compressional and shear velocities of sound at a reference temperature and ultrasonic pulse-repetition-frequencies f_j corresponding to these velocities as a function of pressure (also at the reference temperature) yield the values of $\{dM_j/dp\}_{p=0}$.

The use of equation (1) for porous materials involves a two-step correction. The first correction is for crack-pores. The elastic properties, if measured on a polycrystalline sample, are the apparent properties of the sample; they may or may not correspond to the intrinsic elastic properties of the sample being studied. Certain hot-pressed samples often contain microcracks. Effects of these microcracks on the elastic properties of the samples should be given careful attention by the investigator. Helpful references to these effects as observed on rocks are Brace (1965) and Walsh (1965). The most practical method for finding the intrinsic elastic properties of such samples is to measure both P and S velocities as a function of hydrostatic pressure to about 7 to 10 kb. From these $V_j(p)$ data, velocities at zero-pressure are found by extrapolating high-pressure results back to the zero-pressure point. These velocities found at the origin present crack-free but not pore-free values; isotropic elastic properties at zero-porosity can be evaluated from these data.

The second correction is concerned with pores in the samples and their rate of change with pressure. It was observed that the quantity R_j in the second term of equation (1) is to the first order independent of small porosity at a pressure range of 2 to 10 kb, a range of pressure most commonly utilized in ultrasonic experiments. Theoretical justification for this observation is difficult, if not impossible, without making assumptions as to size, shape, and orientations of pores in the polycrystalline aggregate. Furthermore, even for a pore-free aggregate, the task of determining the macroscopic state of stress distribution is hopelessly complicated, due to numerous superimposed effects which originate from the properties of the mineral grains and from the boundaries between them. For these reasons, a satisfactory general model for the elasticity of porous materials has not yet been developed, in spite of numerous investigations (see Walsh & Brace (1966) for a review). In an earlier analysis of

spherical pores, based on the work of Walsh & Brace (1966), the author (Chung 1971a) indicated that the quantity $(d\eta/dp)$ estimated at the origin is small and is well within the scatter of most experimental data. Thus, with the experimental quantity R_j determined on a porous sample, one should be able to find the pressure coefficients of compressional (L_s), shear (μ), and adiabatic bulk (K_s) moduli of the non-porous material from equations (2) and (3) below:

$$\left\{\frac{dM_j^\circ}{dp}\right\}_{p=0} = \left\{\frac{M_j^\circ}{3K_T^\circ}\right\}_{p=0} + \left\{M_j^\circ \frac{d}{dp}\ (f_{jp}/f_{j0})^2\right\}_{p=0} \tag{2}$$

$$\left\{\frac{dK_s^\circ}{dp}\right\}_{p=0} = \left\{\frac{dL_s^\circ}{dp}\right\}_{p=0} - \tfrac{4}{3}\left\{\frac{d\mu^\circ}{dp}\right\}_{p=o} \tag{3}$$

where L_s°, μ°, and K_s° are the porosity-corrected values and the superscript (°) refers to the zero-porosity.

In the ultrasonic experiments, in which temperature is a variable, we are interested in both P and S velocities as a function of temperature and their temperature coefficients evaluated at various temperatures. From these data, we find the temperature derivatives of the elastic constants in the usual way:

$$\frac{dM_j}{dT} = 2\rho V_j\left(\frac{dV_j}{dT}\right) - \alpha_v M_j \tag{4}$$

where ρ is the density of sample, V_j is the sound velocity in the jth mode (either P or S mode), and α_v is the coefficient of volume expansion. We used thermal expansion data of Skinner (1966) and unpublished data of Singh & Simmons (1971) throughout this study.

In the first-order approximation for low porosity, the porosity-sensitive polycrystalline elastic constants M_j (where $j = P, S$ as before) can be represented by

$$M_j = M_j^\circ\,(1-k\eta) \tag{5}$$

where η is the porosity and M_j° is the elastic constant of nonporous material given by $M_j^\circ = \rho_0\,(V_j^\circ)^2 = 4\rho_0 l_0^2 f_j^2$. k is a constant (see, for example, a review paper by Walsh & Brace 1966). The temperature derivative of the porosity-sensitive elastic constant is then

$$\frac{dM_j}{dT} = \left(\frac{dM_j^\circ}{dT}\right)(1-k\eta) - M_j^\circ\,(k)\,(d\eta/dT). \tag{6}$$

Since $(d\eta/dT)$ is practically zero, the last term drops out. Thus, from equations (5) and (6), we obtain

$$\frac{d\ln M_j}{dT} = \frac{d\ln M_j^\circ}{dT}. \tag{7}$$

Equation (7) implies that the temperature coefficient of an elastic constant determined on a porous polycrystalline sample can be used to evaluate the elastic constant of the non-porous aggregate (as a function of temperature) simply by interpolating the room-temperature constant of the porous sample to that of the non-porous aggregate.

4. Elastic properties of olivine

4.1. *Variation with pressure*

Table 1 summarizes the primary data obtained from the ultrasonic-pressure experiments for all the olivine samples considered in the present study; an estimated total uncertainty in P and S velocities is indicated. This uncertainty includes estimated experimental errors and variations in velocities due to an apparent anisotropy of the olivine sample. The apparent anisotropy of each sample was observed to be small, possibly due to the method of sample preparation (see Cl, p. 7354). The uncertainty in the values of $(f_{jp}/f_{j0})^2$ corresponds to the standard deviation from the weighted least square fit to the experimental data. Fig. 1 shows a variation of $(f_{jp}/f_{j0})^2$ with pressure for olivines by varying the Fe/(Mg+Fe) ratio. It is seen here that the iron substitution for magnesium in the olivine lattice is more sensitive to the pressure variation of S waves than for P waves. From the experimental data in Table 1 applied to the procedure described in the earlier section, values of the first pressure derivative of the elastic constants for various olivines are found. These values are tabulated in Table 2. Also entered in Table 2 are the pressure derivatives of both P and S velocities which were calculated in the usual way. Fig. 2 shows a variation of the pressure coefficients of P and S velocities for olivine as a function of molar percentage fayalite in olivine. Using the criteria defined by Chung (1968, p. 417), these pressure coefficients of the elastic constants should hold to pressures of about $0{\cdot}1\,K_T$ (thus corresponding to a depth of about 360 km); any further extrapolation is unjustifiable.

The pressure coefficient of P velocity changes very little with the iron substitution for magnesium in the olivine lattice. As seen in Fig. 2, the coefficient varies linearly from $1{\cdot}2\,\mathrm{mb}^{-1}$ for forsterite to $1{\cdot}33\,\mathrm{mb}^{-1}$ for fayalite. The iron substitution for magnesium significantly affected the pressure coefficient of the S velocity. The coefficient is $0{\cdot}8\,\mathrm{mb}^{-1}$ for forsterite, and for fayalite it becomes about $0{\cdot}2\,\mathrm{mb}^{-1}$. This variation with increasing iron content is greater than that assumed in many geophysical discussions of the mantle. The apparent reduction in the value of $(d\,\ln V_s/dp)$ of about

Table 1

Composition and measured properties of various olivine samples from ultrasonic-pressure experiments (at 296° K)

Olivine composition, mole (%)	Sample density, g cm^{-3}	Porosity, (%)	Compressional velocity, V_p, km s^{-1}	Shear velocity, V_s, km s^{-1}	$(f_p/f_{p0})^2$ (evaluated at 10 kb)	$(f_s/f_{s0})^2$ (evaluated at 10 kb)
100 Fo	3·164	1·65	8·459 (± ·040)	4·938 (± ·018)	1·02941 (± ·00017)	1·02059 (± ·00010)
95 Fo	3·176	2·98	8·287 (± ·046)	4·823 (± ·020)	1·02965 (± ·00021)	1·02051 (± ·00011)
90 Fo	3·270	1·90	8·226 (± ·033)	4·769 (± ·019)	1·03004 (± ·00018)	1·02066 (± ·00011)
85 Fo	3·386	2·83	8·088 (± ·047)	4·676 (± ·018)	1·03005 (± ·00019)	1·02046 (± ·00011)
80 Fo	3·365	2·19	8·017 (± ·039)	4·615 (± ·016)	1·03009 (± ·00016)	1·01929 (± ·00010)
50 Fo	3·732	1·80	7·454 (± ·037)	4·178 (± ·017)	1·03079 (± ·00019)	1·01681 (± ·00012)
100 Fa	4·287	2·41	6·502 (± ·033)	3·421 (± ·015)	1·03212 (± ·00018)	1·00982 (± ·00012)

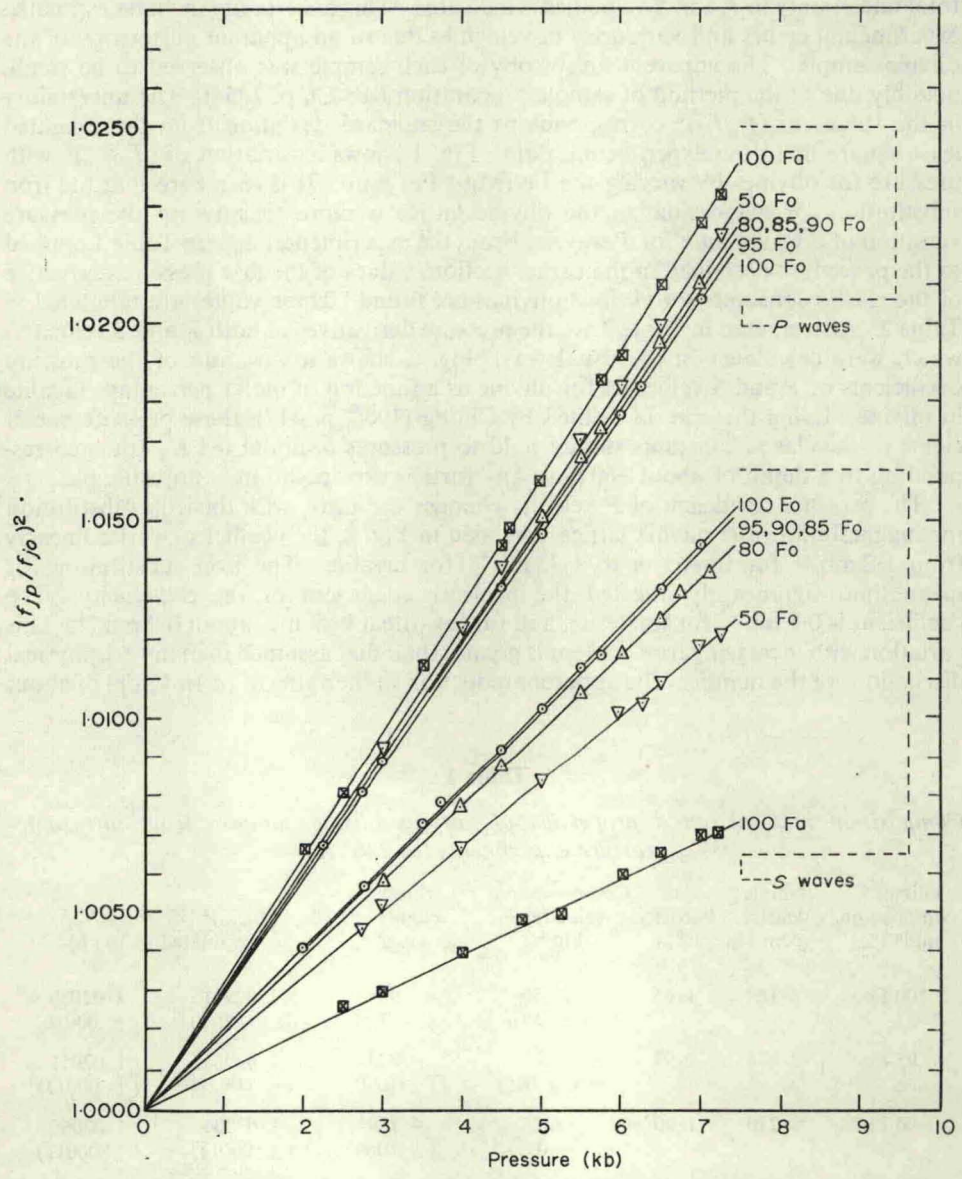

FIG. 1. Variation of frequency-ratio-squared $(f_{jp}/f_{j0})^2$ with hydrostatic pressure and (Fe/Mg) ratio in olivine.

Table 2

Elastic parameters and their pressure and temperature derivatives of olivine as a function of (Fe/Mg) Ratio (at 296° K)

		Olivine composition, mole %							Estimated uncertainty,
Property†	Unit	100 Fo	95 Fo	90 Fo	85 Fo	80 Fo	50 Fo	100 Fa	%
ρ_0	g cm^{-3}	3·217	3·273	3·330	3·386	3·440	3·800	4·393	±0·2
m	g	20·12	20·58	21·00	21·48	21·93	24·60	29·10	±0·2
V_p	km s^{-1}	8·534	8·422	8·317	8·216	8·116	7·534	6·637	±0·5
V_s	km s^{-1}	4·977	4·892	4·815	4·739	4·663	4·213	3·494	±0·5
ϕ	(km s^{-1})J	39·8	39·0	38·3	37·6	36·9	33·1	27·8	±1·1
σ_s	None	0·242	0·245	0·248	0·251	0·254	0·273	0·308	±1·2
L_s	mb	2·343	2·322	2·303	2·286	2·266	2·157	1·935	±0·8
μ	mb	0·797	0·783	0·772	0·760	0·748	0·674	0·536	±0·9
K_s	mb	1·281	1·277	1·274	1·272	1·269	1·258	1·220	±1·8
K_T	mb	1·270	1·266	1·263	1·261	1·258	1·248	1·211	±2·0
dL_s/dp	None	7·51	7·50	7·52	7·47	7·42	7·18	6·75	±3·0
$d\mu/dp$	None	1·85	1·81	1·80	1·76	1·64	1·31	0·62	±3·0
dK_s/dp	None	5·04	5·08	5·13	5·13	5·23	5·44	5·92	±5·0
dK_T/dp	None	5·07	5·11	5·16	5·16	5·27	5·48	5·97	±5·3
$d\sigma_s/dp$	mb^{-1}	0·33	0·33	0·36	0·36	0·40	0·46	0·62	±8·0
dV_p/dp	(km s^{-1})/mb	10·3	10·3	10·3	10·2	10·1	9·5	8·8	±3·0
dV_s/dp	(km s^{-1})/mb	3·8	3·7	3·7	3·6	3·3	2·4	0·6	±3·0
dL_s/dT	kb/°K	−0·296	−0·294	−0·293	−0·292	−0·291	−0·284	−0·273	±2·0
		(−0·360)‡	(−0·357)	(−0·355)	(−0·352)	(−0·350)	(−0·336)	(−0·312)	±2·0
$d\mu/dT$	kb/°K	−0·124	−0·123	−0·122	−0·122	−0·120	−0·113	−0·100	±2·0
		(−0·140)‡	(−0·140)	(−0·139)	(−0·138)	(−0·138)	(−0·132)	(−0·120)	±2·0
dK_s/dT	kb/°K	−0·131	−0·131	−0·132	−0·132	−0·133	−0·135	−0·138	±2·0
		(−0·180)‡	(−0·179)	(−0·177)	(−0·176)	(−0·175)	(−0·168)	(−0·155)	±2·0
$d \ln V_p/dT$	10^{-6}/°K	−50·2	−50·4	−50·8	−51·2	−51·5	−53·4	−57·0	±3·0
$d \ln V_s/dT$	10^{-6}/°K	−64·6	−65·3	−66·0	−66·6	−67·4	−71·4	−78·9	±3·0
$d\sigma_s/dT$	10^{-6}/°K	9	9	9	10	10	13	17	±6·5
θ_D (elastic)	°K	754	740	727	715	703	633	523	±1·0

† The elastic parameters at ambient conditions are from Table 2 in Cl. It is noted that the density value of the 50 Fo composition in Cl should have been 3·800 g cm^{-3} (see Birch 1969, p. 34 and discussion therein).

‡ Data in parenthesis are estimated values at $T = \theta_D$ (see text for description).

75 per cent for fayalite, as compared to forsterite, is noteworthy, since this quantity is closely related to the seismic structure of the upper mantle. We shall return to this subject in a later section.

4.2. *Variation with temperature*

In Table 3, the data obtained from ultrasonic-temperature measurements at 1 bar pressure are tabulated in a convenient form. Combining these data with the elastic constants at ambient conditions, we can evaluate all the first derivatives of the elastic parameters with respect to temperature. Table 2 (18th through 26th rows of this table) summarizes the isobaric temperature derivatives of various elastic parameters, evaluated at 296° K, for olivines in the forsterite-fayalite series.

Values of the temperature coefficients of the elastic constants vary with temperature. It was observed that these coefficients increased almost linearly with temperature for all the olivine samples. This experimental observation permits the use of the present data for estimating the elastic properties of olivine at high temperatures. At high temperatures (where $T \geqslant \theta_D$), the elastic constants of crystalline solids decrease almost linearly with temperature, and their gradient with temperature approaches a constant value. The values in parentheses entered in Table 2 are these high-temperature values of the isobaric temperature derivatives of the elastic constants, evaluated at the Debye temperature of olivine; these high-temperature values should be of more interest to geophysics in the discussions of the Earth's mantle than those values evaluated at the ambient temperature.

Fig. 4 shows values of the temperature derivatives of the elastic constants of olivine as a function of Fe/(Mg+Fe) ratio. It is seen that values of both (dL_s/dT) and $(d\mu/dT)$ decrease with increasing the Fe/(Mg+Fe) ratio in olivine. Effects of this Fe/(Mg+Fe) ratio on the (dK_s/dT) value are seen to be small; at 300° K, for example,

Table 3

Variation of density, shear modulus, and adiabatic bulk modulus of olivine with temperature (at one bar)

Property	Temperature °K	Olivine composition, mole %						
		100 Fo	95 Fo	90 Fo	85 Fo	80 Fo	50 Fo	100 Fo
ρ_0, g cm^{-3}	296	3·217	3·273	3·330	3·386	3·440	3·800	4·393
$\mu°$, mb	296	0·797	0·783	0·772	0·760	0·748	0·674	0·536
$K_s°$, mb	296	1·281	1·277	1·274	1·272	1·269	1·258	1·220
$\rho(T)/\rho_0$	273	1·0005	1·0005	1·0005	1·0005	1·0005	1·0004	1·0004
	350	0·9982	0·9982	0·9982	0·9983	0·9983	0·9984	0·9986
	400	0·9965	0·9966	0·9967	0·9968	0·9969	0·9971	0·9973
	450	0·9947	0·9948	0·9949	0·9951	0·9953	0·9956	0·9958
$\mu(T)/\mu°$	273	1·0023	1·0023	1·0023	1·0023	1·0023	10··22	1·0021
	350	0·9920	0·9922	0·9924	0·9927	0·9930	0·9936	0·9943
	400	0·9838	0·9840	0·9843	0·9846	0·9850	0·9862	0·9880
	450	0·9758	0·9762	0·9766	0·9770	0·9774	0·9789	0·9811
$K_s(T)/K_s°$	273	1·0024	1·0024	1·0024	1·0024	1·0023	1·0022	1·0021
	350	0·9941	0·9941	0·9941	0·9941	0·9941	0·9941	0·9942
	400	0·9880	0·9880	0·9880	0·9880	0·9880	0·9881	0·9883
	450	0·9816	0·9816	0·9817	0·9818	0·9818	0·9820	0·9822

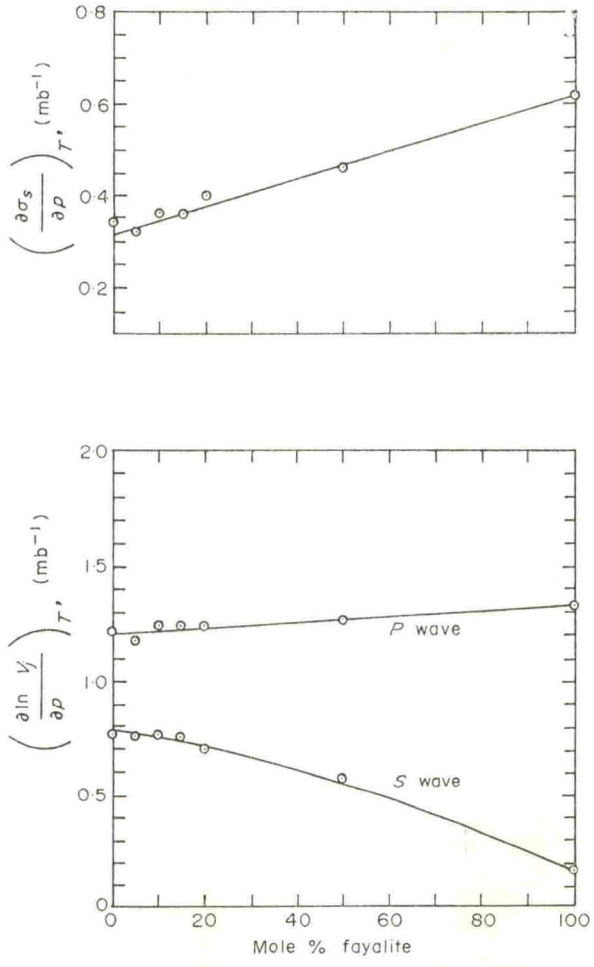

FIG. 2. Pressure coefficient of *P* and *S* wave velocities and pressure derivative of Poisson's ratio as a function of (Fe/Mg) ratio in olivine.

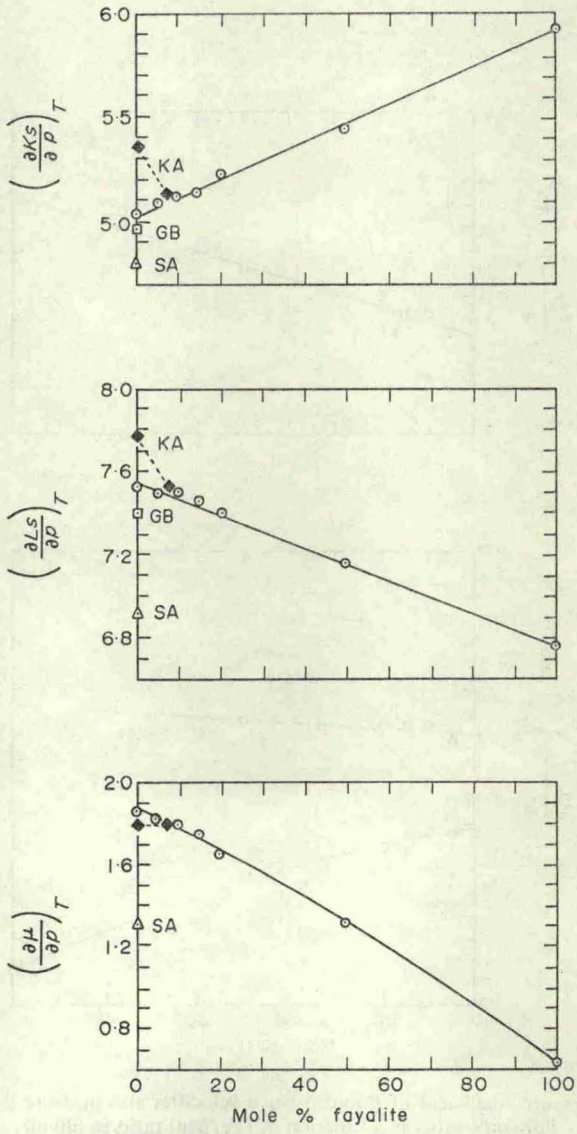

FIG. 3. Pressure derivatives of compressional modulus L_s, shear modulus μ, and the adiabatic bulk modulus K_s of olivine as a function of (Fe/Mg) ratio; comparison with literature data. (△) indicates the datum of Schreiber & Anderson (SA, 1967), (⊡) indicates the datum of Graham & Barsch (GB, 1969), and (◆) indicates the data points of Kumasawa & Anderson (KA, 1969); (⊙) are the present work.

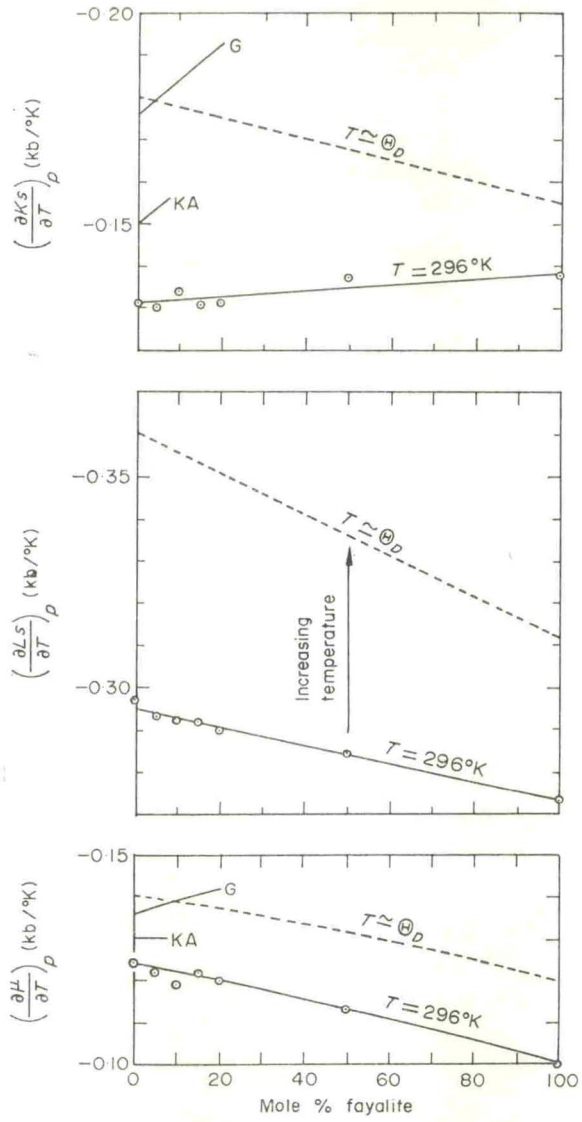

FIG. 4. Variation of temperature derivatives of the elastic constants of olivine with (Fe/Mg) ratio. High-temperature values evaluated at the Debye temperature of each olivine are indicated with a dotted line. (G) stands for Graham's (1970) work and (KA) indicates work of Kumasawa & Anderson (1969); (⊙) are the present work.

the (dK_s/dT) value of forsterite is $-0{\cdot}131$ kb/° K, and for fayalite the (dK_s/dT) value is $-0{\cdot}138$ kb/° K.

Whether an elastic constant is a unique function of volume or not is an important question often asked by geophysicists. The answer to this question forms a basis of the so-called 'Law of Corresponding State' in thermodynamics of solids. An important consequence of the elasticity data reported here is that we can examine the above question in a systematic manner. The elastic constant M_j of olivine can be treated as a function of volume (thus interatomic separation) and temperature.

$$M_j = M_j(V, T)\,. \tag{8}$$

Taking logarithms and differentiating both sides with respect to temperature and rearranging the results, we find

$$\text{(total)} = \text{(implicit)} + \text{(explicit)}$$

$$\frac{d \ln M_j}{dT} = -\alpha_v K_T \left(\frac{\partial \ln M_j}{\partial p}\right)_T + \left(\frac{\partial \ln M_j}{\partial T}\right)_V. \tag{9}$$

Hence, from the present data on both the pressure and temperature derivatives of the elastic constants, we should be able to separate out the *changes* due to temperature from those due to volume. Table 4 lists the pressure and temperature coefficients of compressional (L_s) and shear (μ) moduli along with those of the adiabatic bulk modulus (K_s). The quantities of interest here are $(\partial \ln M_j/\partial T)_V$ which are found from our experimental data; they are listed in the last column of Table 4. If the elastic constants are a function of volume alone, i.e. $M_j = M_j(V)$, then we would expect the quantity represented by the explicit term to be zero. But it is evident from Table 4 that this explicit term is a non-zero value implying the elastic constants are not a function of volume alone.* Most crystalline solids of geophysical interest

Table 4

Test on the volume-dependence Hypothesis of the elastic constants (at 296° K)

Olivine composition, mole %	α_v 10^{-5}/°K	M_j	$\frac{d \ln M_j}{dT}$ 10^{-5}/°K	$\alpha_v K_T \left(\frac{\partial \ln Mi}{\partial p}\right)_T$ 10^{-5}/°K	$\left(\frac{\partial \ln Mi}{\partial T}\right)_V$ 10^{-5}/°K
100 Fo	2·55	L_s	−12·6	+10·4	− 2·2
		μ	−15·6	+ 7·5	− 8·1
		K_s	−10·2	+12·7	+ 2·5
50 Fo	2·43	L_s	−13·1	+10·1	− 3·0
		μ	−16·8	+ 5·9	−10·9
		K_s	−11·0	+13·1	+ 2·1
100 Fa	2·40	L_s	−13·9	+10·2	− 3·7
		μ	−18·3	+ 3·4	−14·9
		K_s	−11·3	+14·1	+ 2·8

*Geophysical literature concerned with the elasticity often assumes the elastic constants are a function only of volume, but this is clearly incorrect. Anderson & Nafe (1965, p. 3959) found a relationship between the shear modulus and volume for oxide compounds, but this correlation seen by these authors should be re-examined before being accepted. The elastic constants of most alkali halides in which there are prominent central forces between the constituent ions can be treated as a unique function of volume only, as was first demonstrated by Lazarus (1949). A direct translation of this picture of the alkali halides to the system of oxides and silicates is dangerous and often misleading.

possess non-centrosymmetric structures. The elastic constants of such solids as olivine, for example, depend also on the electronic polarizabilities of the constituent ions; hence, their variations with pressure and temperature are sensitive to how the polarizabilities are affected by these thermodynamic variables. The quantity represented by the implicit term in equation (9) is thus a measure of the contribution from these electronic polarizabilities, as well as that arising from lattice vibrations of the constituent ions in olivine. The role of these polarizabilities is particularly important for understanding the constitution of the seismic structure and the electrical properties of the mantle.

4.3. *Discussion of literature data*

The present data on the elasticity of olivine may be related to some other data already found in a number of geophysical manuscripts. This discussion is essential since some data strongly oppose others. Many authors, however, use data now believed to be ' questionable ' in geophysical and geochemical theories and experiments.

Experimental data on the elastic properties of olivine come from several distinctively different sources: (1) from the velocity measurements on ultrabasic rocks, typified by the work of Birch (1960, 1961a), Simmons (1964), Christensen (1966a, 1966b), and Mao *et al.* (1970); (2) from the systematic determinations of the elastic constants of gem-quality olivine single-crystals, typified by the work of Verma (1960), Kumasawa & Anderson (1969), and Graham & Barsch (1969); and (3) from the velocity measurements on synthetic polycrystalline olivine aggregates, typified by the work of Schreiber & Anderson (1967) and Chung (1970). Recently, Fujisawa (1970) and Graham (1970) also performed velocity measurements on an aggregate sample of olivine. Of course, much information about compressibility of olivine comes from a study of pressure effects on volume of olivine samples, work of a kind performed by Adams (1931), Bridgman (1948), and more recently Takahashi (1970) and Olinger & Duba (1971). Shock compression of olivine, as performed by McQueen *et al.* (1967) and Ahrens, Lower & Lagus (1971), provides further information on the compressibility of this material at very high pressures.* In the earlier report (see C1; Table 3, and discussion on page 7356), a systematic comparison and discussion was given of these elasticity data at ambient conditions. The following summary can be made. The present elasticity data of olivine are in general agreement with most of the literature data cited above. Exceptions to this agreement are those data reported by Adams (1931), Schreiber & Anderson (1967), Soga & Anderson (1967), and Graham (1970). The writer believes Adams' bulk modulus for fayalite is about 10 per cent too small, Graham's shear modulus for fayalite is about 30 per cent too big,† and the bulk modulus value reported by Soga & Anderson and Schreiber & Anderson for forsterite is about 25 per cent too small. The large differences noted for data of Soga & Anderson and Schreiber & Anderson are probably due to porosity in their samples.

Table 5 tabulates and compares all the experimental data found in the literature to date for the pressure and temperature derivatives of the elastic constants of olivine with the present data. (It may be noted that some elasticity data estimated or extra-

*It is noted that neither the isothermal compression nor the shock compression studies provide information about the behaviour of shear waves. The use of these compression data alone cannot described the elasticity of the compressed materials completely. In addition, the compression data direct their emphasis to the compliance property like compressibility, whereas the ultrasonic elasticity data direct emphasis toward the stiffness property such as the adiabatic bulk modulus and shear modulus.

†Graham's (1970) elasticity data ($K_s = 1{\cdot}060$ mb and $\mu = 0{\cdot}688$ mb) have been revised in personal communications to give $K_s = 1{\cdot}202$ mb and $\mu = 0{\cdot}560$ ($\mp 0{\cdot}8$ per cent) mb. These revised data of Graham agree favourably with those reported by Chung (1970, Table 2).

Table 5

Experimental bulk modulus and shear modulus for various olivines and their pressure and temperature derivatives; Comparison with literature data (evaluated at zero-pressure and 296° K)

Olivine composition mole %	ρ g cm^{-3}	μ mb	K_s mb	$\frac{d\mu}{dp}$	$\frac{dK_s}{dp}$	$\frac{d\mu}{dT}$ kb/°K	$\frac{dK_s}{dT}$ kb/°K	Reference
100 Fo	3·021	0·574	0·974	1·3	4·8	—	—	Schreiber & O. L. Anderson (1967)
100 Fo	2·996	0·5869	0·9641	—	—	−0·11	−0·13	Soga & O. L. Anderson (1967)
100 Fo	3·224	0·811	1·286	1·80	5·37	−0·130	−0·150	Kumasawa & O. L. Anderson (1969)*
100 Fo	3·222	0·816	1·296	1·82	4·97	−0·136	−0·176	Graham & Barsch (1969)*
100 Fo	3·217	0·797	1·281	1·85	5·04	−0·12	−0·13	This work
95 Fo	3·273	0·783	1·277	1·81	5·08	−0·12	−0·13	This work
93 Fo	3·331	0·791	1·294	1·79	5·13	−0·130	−0·156	Kumasawa & O. L. Anderson (1969)*
90 Fo	3·330	0·772	1·274	1·80	5·13	−0·12	−0·13	This work
85 Fo	3·386	0·760	1·272	1·76	5·13	−0·12	−0·13	This work
80 Fo	3·440	0·748	1·269	1·64	5·23	−0·12	−0·13	This work
50 Fo	3·800	0·674	1·258	1·31	5·44	−0·11	−0·14	This work
100 Fa	4·393	0·536	1·220	0·62	5·92	−0·10	−0·14	This work

* VRH values from single-crystal data.

polated from various assumptions, such as those of Schreiber (1969) and Graham (1970, p. 287 and 288), could not be listed in Table 5.) Included in the comparison are the single-crystal forsterite data (VRH values) of Kumasawa & Anderson (1969) and Graham & Barsch (1969) and polycrystalline forsterite data of Soga & Anderson (1967) and Schreiber & Anderson (1967). The single-crystal peridot data (VRH values) of Kumasawa & Anderson (1969) are also entered in Table 5. Considering the experimental errors involved in each set of these elasticity data, there is general agreement for most of the pressure derivative data for forsterite and peridot. In particular, the present data agree very well with forsterite data of Graham & Barsch (1969, p. 5955), and also with peridot data of Kumasawa & Anderson (1969, p.5970). It seems, however, that the $(d\mu/dp)$ value originally reported by Schreiber & Anderson (1967, p. 763) and later summarized by Anderson *et al.* (1968, p. 494, Table 1) is about 30 per cent too small when compared with most other data. Table 5 also indicates that the (dK_s/dp) value for forsterite reported by Kumasawa & Anderson 1969, p. 5970) seems rather high (considering the experimental accuracy stated therein). Furthermore, the elasticity data of these authors for their forsterite and peridot shows that the bulk modulus increases slightly with increasing iron content in the olivine samples. The present work, as summarized in Table 2 and also in Fig. 3, shows an increase of (dK_s/dp) with increasing Fe/(Mg+Fe) ration in the forsterite-fayalite series. Our data also show that this (dK_s/dp) increase with the iron content in the olivine lattice is accompanied by a slight decrease in the bulk modulus of olivine. The bulk modulus and its pressure derivature are important parameters entering into solid equations of state and thermodynamics of these solids. The change of these parameters with the iron content in olivine should be understood, therefore, if the physical state and chemical composition of the Earth's mantle is to be correctly characterized.

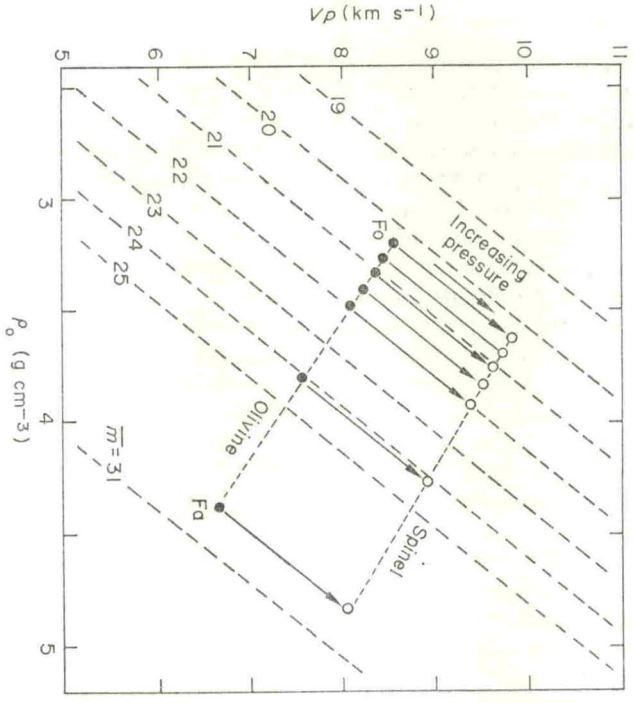

FIG. 5(a). Compressional wave velocity-density-mean atomic weight relation for olivine. The contours of $\bar{m}$ are drawn from Birch's law. The closed circles represent experimental quantities and the open circles show estimated values for the olivine-transformed spinels.

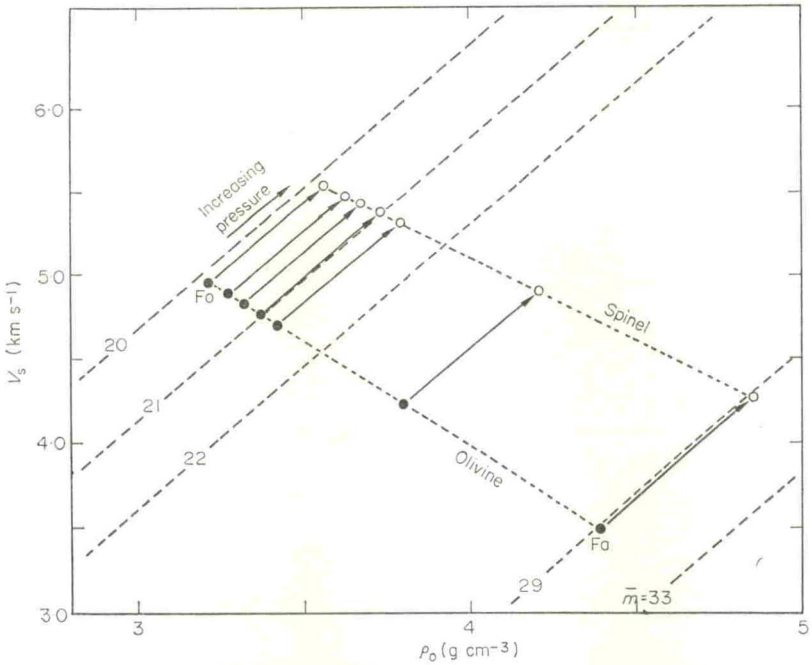

FIG. 5(b). Shear wave velocity-density-mean atomic weight relation for olivine. The closed circles are the present experimental data; the open circles represent estimated values for the olivine-transformed spinels.

Generalization and discussion

As concluded in the previous paper (Chung 1970), the iron substitution for magnesium in the olivine lattice results in a systematic decrease in the velocity of both P and S waves. Iron increases the density but slightly reduces the bulk modulus of olivine, thus making an iron-rich olivine slightly more compressible. The bulk modulus is inversely proportional to volume, as was discussed by Anderson & Nafe (1965) and Knopoff (1967). The mean atomic volume defined by $(\overline{m}/\rho)$ for fayalite is 6·624 cm^3, whereas forsterite is 6·254 cm^3; for fayalite in comparison with forsterite, there is a 4·7 per cent reduction in the bulk modulus, and this is consistent with about 5 per cent increase in the olivine volume.

The velocities of the compressional and shear waves in olivine are plotted respectively in Fig. 5(a) and (b) as a function of density and also of the Fe/(Mg+Fe) ratio. The same diagram as Fig. 5(a) has appeared in the earlier report, in which the contours of the mean atomic weight were derived from the well-known Birch's law for the velocity-density-mean atomic weight relation for minerals and rocks. The contours in Fig. 5(b) were drawn in a similar way from the shear velocity–density line for $\overline{m} = 21$, based on work of Simmons (1964), Kanamori & Mizutani (1965), and Christensen (1966a, b). Christensen (1968) established similar contours and found a relation that $V_s = 1{\cdot}63\rho - 0{\cdot}88$, where V_s is in (km s^{-1}) and ρ in (g cm^{-3}). The velocity of the bulk waves (frequently called ' hydrodynamical waves ') as a function of density and mean atomic weight is plotted in Fig. 5(c), in which the contours were drawn from the calculated bulk velocity–density for rocks and minerals based on the velocity measurements of Birch (1960, 1961a), Simmons (1964), Kanamori & Mizutani (1965), and Christensen (1966a, b). These calculated data points establishing the contours of Fig. 5 are omitted from the diagrams so that the present olivine data alone can be clearly illustrated.

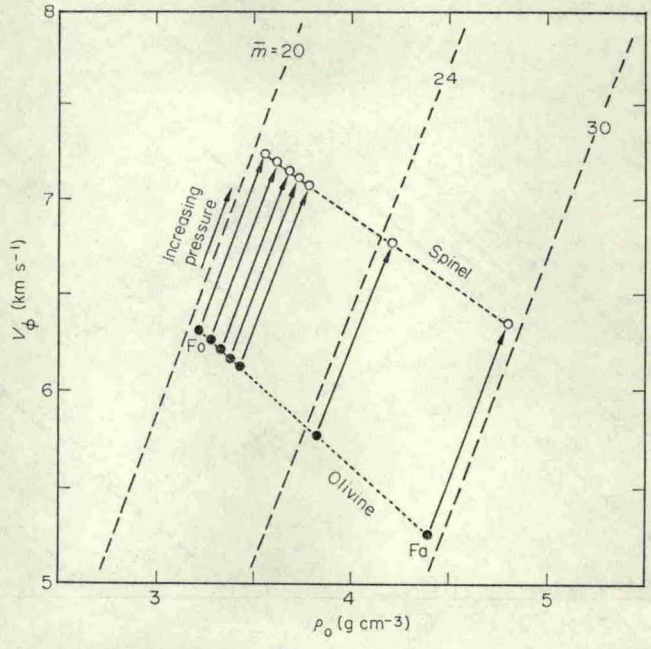

FIG. 5(c). Bulk sound velocity-density- mean atomic weight relation for olivine. The closed circles are the present experimental data; the open circles represent estimated values for the olivine-transformed spinels.

Under pressure, the density of an olivine with a specific Fe/(Mg+Fe) ratio would increase through a gradual decrease in mean atomic volume. Application of pressure to the olivine will increase the sound velocities (V_p, V_s, and V_ϕ) and these velocities (interpolated to the zero-pressure point) will follow along the line of constant mean atomic weight. This trend is shown with arrows in Fig. 5. The significance of Fig. 5 can be illustrated by the two examples below. First, using these diagrams, a velocity-density distribution for an '*olivine upper mantle*' may be estimated, with an assumption that the changes of mean atomic weight in the upper mantle are associated with variations in the Fe/(Mg+Fe) ratio in olivine alone. Second, velocities of the elastic waves in the high-pressure form of olivine can be estimated from these figures.

Change of the Fe/(Mg+Fe) ratio from 0·1 to 0·3 (corresponding to mean atomic weights of 21·0 to 22·8) would produce a decrease in the compressional velocity of 0·32 km s^{-1} and an increase in the olivine density of about 0·25 g cm^{-3}. Similarly, for the shear wave velocity, we find that a change in the Fe/(Mg+Fe) ratio from 0·1 to 0·3 in the upper mantle would result in a decrease in the shear wave by about 0·28 km s^{-1} with a density increase of about 0·25 g cm^{-3}. In the same way, the velocity of the bulk waves (V_ϕ) will decrease by about 0·22 km s^{-1}. In the upper mantle, recent progress in geophysical theories leads us to believe that the mean atomic weight increases with depth to about 22 or slightly higher (see Press 1970b); this implies chemical changes taking place in the upper mantle structure. It is likely that this increase of the mean atomic weight in the upper mantle is also associated with iron enrichment in pyroxene, garnet, and olivine. Effects of iron on the elastic properties of pyroxene and garnet are presently under investigation. Our preliminary results suggest that the actual Fe/(Mg+Fe) ratio of olivine in the upper mantle is approximately 0·13. A more conclusive discussion on this subject will follow in a later communication as the elasticity data on pyroxene and garnet as a function of iron content become available.

With an increased density of about 10 per cent, olivine transforms into a spinel structure at high pressure (see Ringwood (1970) for a recent review). Mizutani *et al.* (1970) successfully prepared a fayalite-transformed spinel sample and measured the compressional velocity as a function of pressure to about 6 kb. They found the compressional velocity in the spinel form of Fe_2SiO_4 is 8·05 km s^{-1} at ambient conditions. This value is about 21 per cent greater than that of fayalite. The datum of Mizutani *et al.* (1970) is plotted in Fig. 5(a). Note that this datum point meets at the intercept of the two lines drawn from the density and the mean atomic weight. Both D. L. Anderson and O. L. Anderson in their respective presentations at the Birch Symposium in April, 1970 (to be published), made similar observations. Incorporating Mizutani *et al's* datum with assumptions, Liebermann (1970) in his recent paper also made a similar observation. If one assumes that the olivines of other compositions behave similarly, a series of lines parallel to a specific mean atomic weight characterized by the Fe/(Mg+Fe) ratio in the olivine composition can be drawn as before (see C1, Fig. 1). Knowing the end-point density of the spinel of the given composition, one can estimate its velocity. In this manner velocities of the compressional and shear waves in the spinel phase of $(Mg_x\,Fe_{1-x})_2SiO_4$ may be found; they are identified by open circles in Fig. 5. Table 6 lists these estimated values and compares them with experimental data on olivine. Note that, in every olivine composition considered here, there is an increase in density values of about 10 per cent. These density increases due to the phase change result in about 13 to 21 per cent increase in the compressional wave velocity, about 11 to 22 per cent increase in the shear wave velocity, and about 15 to 20 per cent increase in the bulk sound velocity as the Fe/(Mg+Fe) ratio changes from zero to one.

The bulk modulus changes with the phase change. Since the density of an olivine-transformed spinel increases about 10 per cent, and since, according to Anderson & Nafe (1965) the bulk modulus is inversely proportional to the volume per ion pair,

Table 6

Elastic properties of $(Mg_xFE_{1-x})_2SiO_4$ *before and after the olivine-spinel phase transformation*

+Fe)	Structure and % change	Density, g cm^{-3}	V_p	V_s (km s^{-1})	V_ϕ	ϕ (km s^{-1})^2	μ mb	K_s	
g	Olivine	3·217	8·534	4·977	6·309	39·8	0·797	1·281	
	Spinel†	3·556	9·66	5·54	7·24	52·4	1·09	1·86	
	% Change	10·6	13·3	11·3	14·7	32·0	37	45	−1
	Olivine	3·330	8·317	4·815	6·189	38·3	0·772	1·274	
	Spinel†	3·683	9·49	5·42	7·13	50·9	1·08	1·87	4
	% Change	10·7	14·1	12·4	15·2	33·0	40	47	−1
	Olivine	3·440	8·116	4·663	6·075	36·9	0·748	1·69	
	Spinel†	3·815	9·33	5·29	7·05	49·8	1·07	1·89	
	% Change	10·7	14·6	13·5	16·0	37·0	42	50	−
	Olivine	3·800	7·534	4·213	5·753	33·1	0·674	1·256	
	Spinel†	4·209	8·85	4·92	6·80	46·1	1·02	1·93	
	% Change	10·8	17·6	16·5	18·4	40·0	50	55	−
e	Olivine	4·393	6·637	3·494	5·273	27·8	0·536	1·220	
	Spinel†	4·849	8·05‡	4·28	6·35	40·4	0·89	1·96	
	% Change	10·4	21·1	22·5	20·4	45·0	65	60	−

s (see text).

l by Mizutani *et al.* (1970).

the bulk modulus of the high-pressure phase would be about 10 per cent higher than that of the low-pressure olivine phase. However, as is seen in Table 6, values of the bulk modulus show about a 45 per cent increase for the Mg_2SiO_4 – spinel and a 60 per cent increase for the Fe_2SiO_4 – spinel from the respective bulk moduli in the olivine form.

There seems to be a relationship between the bulk modulus and the volume per atom at zero pressure for all solids. Birch (1961b), Anderson & Nafe (1965), D. L. Anderson (1969), and Knopoff (1967) have investigated such a relationship. The density of the solid depends upon the mean atomic weight ($\overline{m}$) and the mean atomic volume ($\overline{m}/\rho$). The oxygen ions account for most of the volume in olivine. Along a line of constant mean atomic weight (thus the composition remains constant), density changes only through changes of mean atomic volume caused by a change either in pressure or in temperature (or both in the case of the Earth's interior). Since the bulk modulus is related to the inverse of volume, and since by definition the density is proportional to the inverse of volume, there seems to be a definite relationship between the density and the rate of isothermal change of the bulk modulus with pressure (evaluated at zero pressure). Fig. 6 plots this rate of change of the bulk modulus with pressure termed (dK_0/dp) for olivine as a function of density and the Fe/(Mg+Fe) ratio. Application of pressure to olivine will decrease the (dK/dp) value and this (dK/dp) after interpolation to the zero-pressure point will follow along the line of constant mean atomic weight. This trend is illustrated with an *arrow* in the diagram. As olivine becomes a spinel at high pressure, the corresponding value of (dK_0/dp) can be estimated by knowing the density value of the olivine-transformed spinel. These estimated values for (dK_0/dp) are identified by *open circles* in Fig. 6 and entered in the last column of Table 6. These estimated values, although subject to confirmation, provide a basis for specifying equations of state of the olivine-transformed spinels; the equations of state of these spinels are discussed in a subsequent paper (Chung 1971b).

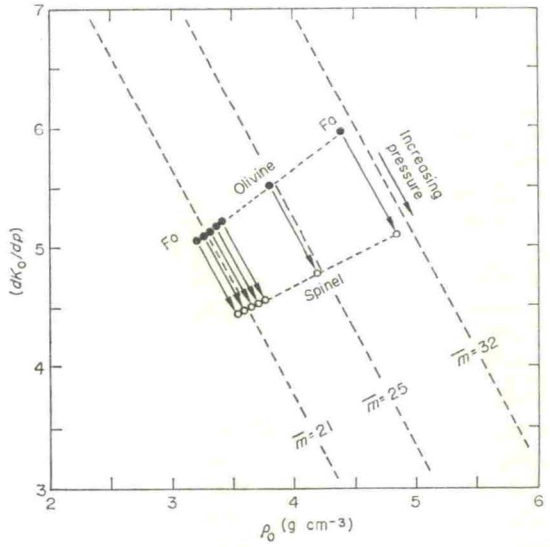

FIG. 6. An empirical relation for dK_0/dp) and density and mean atomic weight in olivine. The closed circles are the present experimental data on olivines; the open circles are estimated values for the olivine-transformed spinels.

5. Equations of state of olivine

5.1. *Variation with (Fe/Mg) Ratio*

The equations of state most widely used in geophysics are those of Murnaghan (1944, 1951) and Birch (1952). Chung, Wang & Simmons (1970), referred to below as CWS, discussed the general superiority of the Birch equation of state over that of Murnaghan with respect to calculation of the density and the seismic parameter from the low-pressure laboratory data. Use of the Murnaghan equation of state leads to overestimates of the density and seismic parameter at high pressures. The reasoning here is associated not only with the Murnaghan assumption of a linear variation of the bulk modulus with pressure but also with an inadequacy of the functional form of the equation itself. In his recent review, Macdonald (1969) presented several other limitations for the use of the Murnaghan equation of state at high pressure; he concluded from thermodynamics that the Murnaghan equation yields a finite negative pressure at which the density approaches a finite value, an unacceptable result. For these reasons, this paper uses the Birch equation in the discussion of equations of state for olivine.

The Birch equation of state is a phenomenological equation based on rapidly converging Taylor expansion of the interatomic potential. The equation was derived from the finite strain theory with cubic and quadratic terms of the Eulerian strain retained in the Helmholtz free energy:

$$p = (3K_0/2)\,(y^7 - y^5)\,[1 + \tfrac{3}{4}(m-4)\,(y^2-1)] \tag{10}$$

where $y = (\rho/\rho_0)^{\frac{1}{3}} = (V_0/V)^{\frac{1}{3}}$. K_0 and m are material parameters corresponding to the isothermal bulk modulus and its first pressure derivative evaluated at zero pressure. (If equation (10) is used in an adiabatic form, as in the calculation of the seismic parameter, K_0 and m are respectively the adiabatic bulk modulus and the adiabatic pressure derivative of the adiabatic bulk modulus).

Values of K_0 and m for olivine as a function of Fe/(Mg+Fe) ratio in the forsterite-fayalite series have been tabulated in Table 2 (under K_T and dK_T/dp). It was seen that K_0 decreases with increasing the Fe/(Mg+Fe) ratio, whereas m increases with an iron enrichment in olivine. Fig. 7 represents, in accordance with equation (10), the relative density-pressure trajectory for olivine by varying the Fe/(Mg+Fe) ratio. Effects of iron substitution in olivine on the olivine equation of state are seen here to be rather small. The iron enrichment in olivine yields a gradual reduction, though small, in the K_0 value, but increases the m value; apparently, in accordance with equation (10), these K_0 and m work in the opposite direction in such a way that the effect of the iron substitution for magnesium on the olivine equation of state is small.

In the following, the density–pressure trajectories calculated from equation (10) are compared with isothermal compression data as well as data on shock-wave compression. Data on the static compression of a fayalite-olivine were first reported by Adams (1931) to about 15 kb and of a peridot-olivine by Bridgman (1948) to about 40 kb. The volume compression of olivine has been determined recently from X-ray measurements of the lattice parameters to about 120 kb by Olinger & Duba (1970) and by Takahashi (1970) for a fayalite-olivine to about 150 kb. McQueen, Marsh & Fritz (1967) and Ahrens *et al.* (1971) presented the shock-compression data of various olivines to several hundreds of kilobars. Rigorously speaking, the shock-compression data cannot be directly compared with data on the isothermal compression resulting from the static volume measurements with pressure. Nor can they be directly compared with the density–pressure trajectories resulting from the isothermal form of equation (10). The shock-wave measurements result in adiabatic quantities, whereas the static compressions give the isothermal values; the proper comparison of these compression data with the density–pressure trajectories resulting from a particular equation of state must in principle include an adiabatic-isothermal correction.

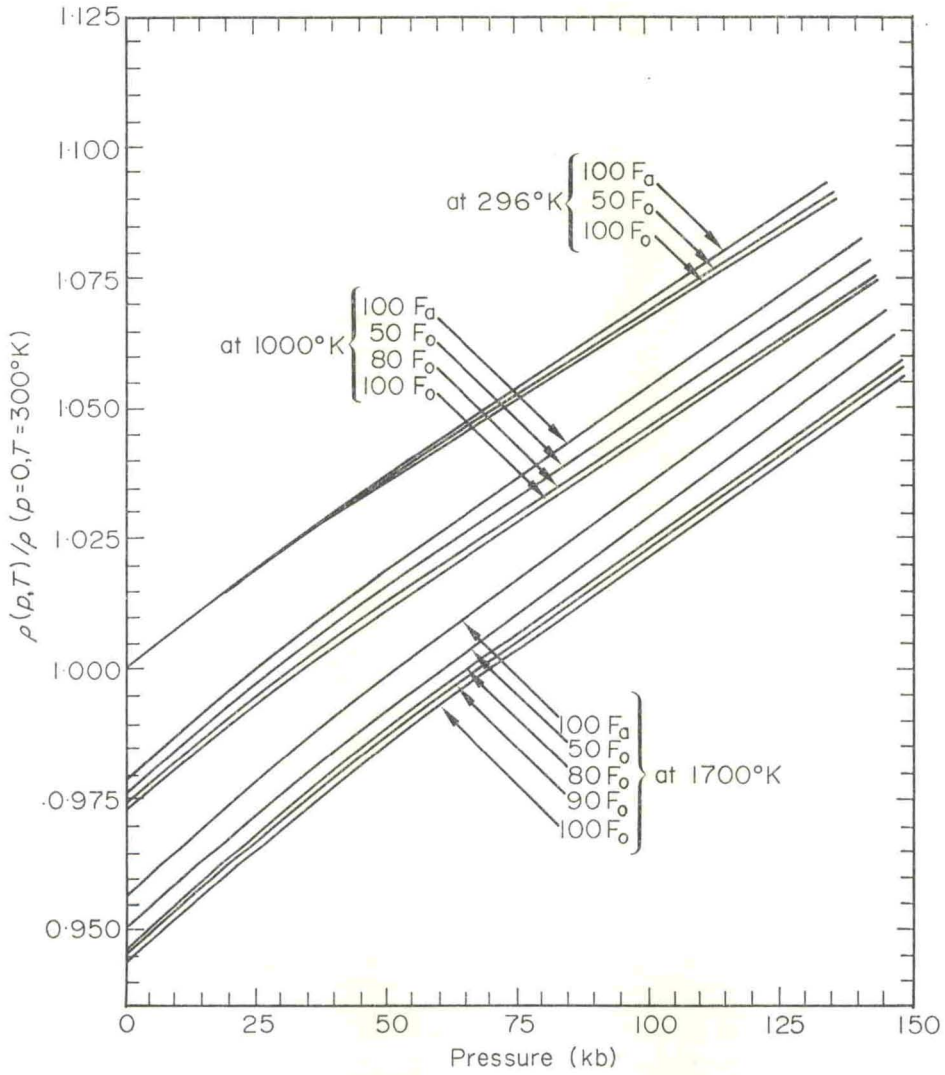

FIG. 7. The density–pressure trajectories of olivines with different (Fe/Mg) ratios at three different temperatures; an illustration of the '*critical pressure* p_{cr}' (defined in the text) of olivines.

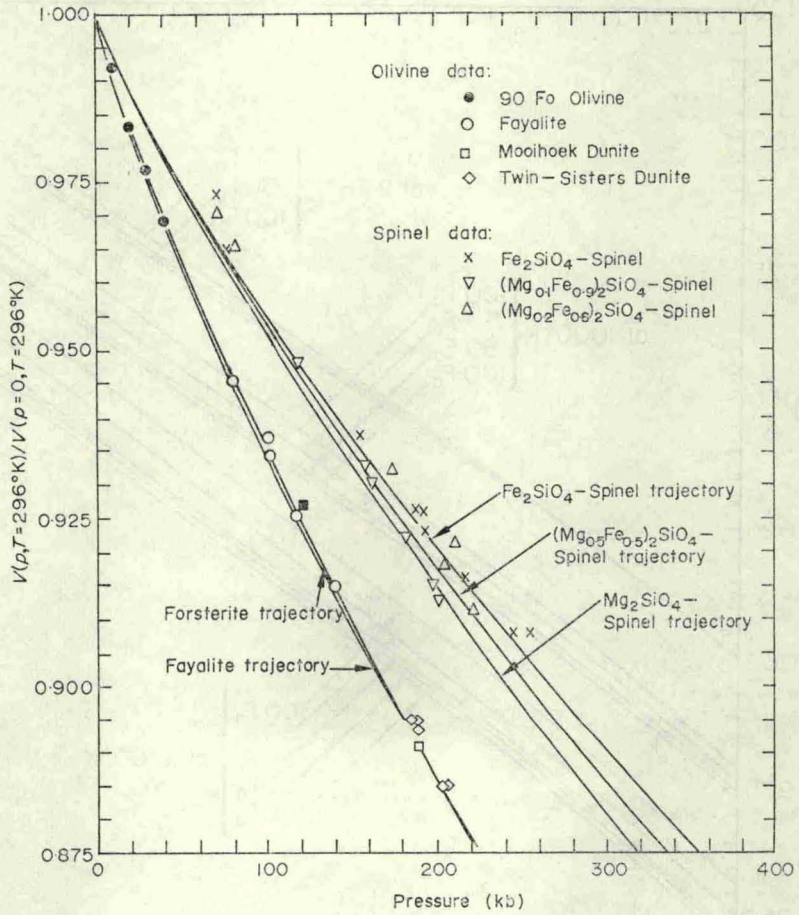

FIG. 8. Comparison of the calculated pressure–volume relation of olivine with experimental compression data. The solid lines are the present work, independent of compression data points. The isothermal compression data of olivine are due to Bridgman (●) and to Takahashi (○). The shock compression data are due to McQueen, Marsh, & Fritz for Mooihoek dunite (□) and Twin-Sisters dunite (■). The isothermal compression data of olivine-transformed spinels are due to Mao *et al.* (1969), and the solid lines are the calculated pressure-volume relation for the olivine-transformed spinels in the Mg_2SiO_4-Fe_2SiO_4 series established by Chung (1971b).

For olivine, this correction is found to be small, as compared with experimental errors involved in the K_0 and m values, and is therefore neglected for present purposes.

The calculated volume-pressure trajectories for 100Fo and 100Fa olivines are compared with compression data in Fig. 8. The compression data entered here are those of Bridgman, Takahashi, and McQueen *et al.*; it is seen that the trajectories compare very well with these compression data.

5.2. *Variation with temperature*

Pressure increases the density of olivine, but temperature reduces it; thus there is a critical pressure p_{cr} defined by the pressure, for a given temperature, at which

$$\rho\,(p_{cr}, T) = \rho(p = 0, T = RT)$$

RT refers to an ambient reference temperature. At p_{cr}, temperature effects on density cancel the pressure effects completely. Below p_{cr}, temperature effects on the density dominate over the pressure effects, and above p_{cr} the pressure effects dominate over the temperature effects on the density of the solid. This critical pressure for olivines with different Fe/(Mg+Fe) ratios can be estimated from data on thermal expansion and compression ratio resulting from the equation of state (10) by

$$p_{cr}(T) = K_T(T)\{(p/K_0)\} \quad \text{at } \rho_0/\rho(T). \tag{11}$$

Values of the critical pressure for olivine at three chosen temperatures (700°, 1000° and 1700°K) are listed in Table 7. For example, at 1000°K, p_{cr} for forsterite is about 34 kb and about 26 kb for fayalite.

The Birch equation of state is isothermal referring to the compression ratio $\rho(p, T)/\rho(p = 0, \quad T = RT)$ and $K_0(p = 0, T)$. Suppose, however, we wish to relate all our compression data to the ambient conditions. Then, in accordance with the procedure described earlier (see CWS, p. 5119), we have

$$\frac{\rho(p,T)}{\rho(p=0,\,T=RT)} = \frac{\rho(p,T)}{\rho(p=0,\,T)} \cdot \frac{\rho(p=0,T)}{\rho(p=0,\,T=RT)} \tag{12}$$

under the assumption that the density ratio given by $\rho(p = 0, T)/\rho(p = 0, T = RT)$ is independent of pressure. (This assumption is a practical one and a good approxima-

Table 7

Relative density and 'Critical' pressure of olivine at three different temperatures

	Temperature,	Olivine composition, mole %					Probable error,
Property†	°K	100 Fo	90 Fo	80 Fo	50 Fo	100 Fa	%
$\rho(p, T)/\rho_0$	700	0·9852	0·9853	0·9861	0·9872	0·9883	1
	1000	0·9732	0·9740	0·9744	0·9763	0·9789	1
	1700	0·9440	0·9450	0·9462	0·9500	0·9560	3
p_{cr}, kb	700	19·5	19·4	18·1	16·7	15·1	2
	1000	33·7	32·5	32·3	29·8	25·6	2
	1700	69·5	67·5	65·2	60·1	51·4	5

† The *critical* pressure referred here to as p_{cr} is defined as the pressure, for a given temperature, at which $\rho(p_{cr}, T) = \rho(0, 296°K)$, and is meant to imply the following: Pressure works in the opposite direction of temperature, but at p_{cr} temperature effects cancel the pressure effects on density. Above this p_{cr}, the pressure effects dominate over the temperature effects in solid.

tion, since a factor of three change in thermal expansion changes the density ratio by less than 1 per cent.) Thus we can obtain $\rho(p, T)/\rho(p = 0, T = RT)$ by multiplying the isothermal compression ratio $\rho(p, T)/\rho(p = 0, T)$ by the constant factor $\rho(p = 0, T)/\rho(p = 0, T = RT)$ obtained from thermal expansion data. The results on two chosen temperatures (1000° and 1700° K) are plotted in Fig. 7. Fig. 7 shows the pressure–dependent density of olivine as a function of temperature and Fe/(Mg+Fe) ratio. It is generally seen that olivines of all the compositions are more compressible at high temperatures. It is also seen that the greater the Fe/(Mg+Fe) ratio in olivine the more compressible the olivine becomes at all temperatures.

6. *Application to the Earth*

The elasticity data presented in this paper may aid discussion of the Earth's mantle within a peridotitic model. We have attempted to relate the elasticity data with the bulk sound velocity and density distribution in the Earth's mantle. As noted by Pree (1970b), a comparison of laboratory data with velocity–density distribution of earth models minimizes the errors arising from uncertain temperature distributions in the Earth's interior.

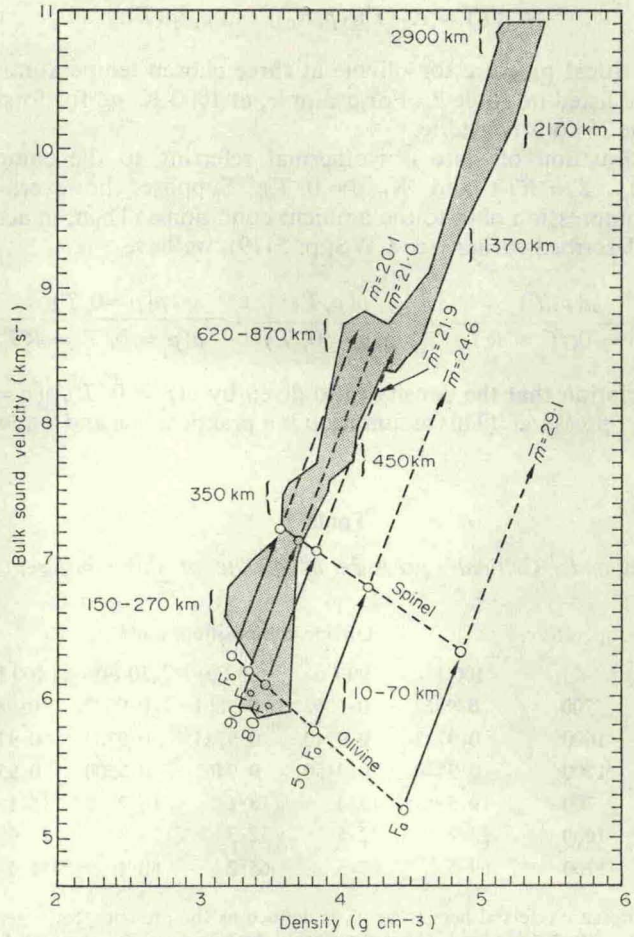

FIG. 9. Comparison of the laboratory V_ϕ—ρ relation for olivine with F. Press's solutions of the Earth data.

In recent years, precise data on travel times for P and S waves, the spatial derivatives of these travel times, the equally accurate eigenperiods of the Earth, as well as surface wave dispersion, have become available (see, for example, Archambeau, Flinn & Lambert (1969), Whitcomb & D. L. Anderson (1970), and Kanamori (1970). The usefulness of these geophysical data has initiated numerous data inversions to obtain the unique elastic wave velocity and density distribution in the Earth. Among the more successful methods are the Monte Carlo techniques to develop families of possible solutions for the entire Earth. Press (1968, 1969, 1970a, b) presented a systematic development of these Monte Carlo solutions and established workable contraints for the earth models. Press (1970b) recently derived successful models for density and elastic wave velocity distributions in the Earth, using oceanic data.

The Monte Carlo solutions for the bulk sound velocity-density relation of the Earth's mantle, presented by Press (1970b), is reproduced in Fig. 9. Fig. 9 compares the density and bulk sound velocities found in this work with Press's solutions. In terms of Press's division of the mantle into three zones, we find for the second zone that the slopes of olivine and olive-transformed spinel with Fe/(Mg+Fe) ratios of about 0·05 to 0·15 are quite similar to large numbers of the Monte Carlo successful solutions in the region 150–870 km. These Fe/(Mg+Fe) ratios correspond to the mean atomic weight $\overline{m}$ of about 20·1 to 21·5 agreeing with the $\overline{m}$ limit set by Press. The olivine-spinel phase change at about 350 km is indicated in the velocity-density plot; the laboratory data on the bulk sound velocity-density plot are in accordance with the result of the Monte Carlo solutions.

If one accepts the present elasticity data as representative of olivine, one must then conclude, within the framework of a peridotitic model, that the olivine has the necessary equation-of-state properties to qualify as a likely candidate for mantle constituents.

Acknowledgments

The author expresses his thanks to Dr Frank Press for discussion and interest shown in this work. I am grateful to Dr Gene Simmons for encouragement and the use of capital equipments.

Financial support of this work was provided by the National Science Foundation Grant GA-11091, which the author gratefully acknowledges.

Department of Earth & Planetary Sciences,
Massachusetts Institute of Technology,
MIT *Room* 54-716
Cambridge, Massachusetts 02139

References

Adams, L. H., 1931. The compressibility of fayalite, and the velocity of elastic waves in peridotite with different iron-magnesium ratio, *Beitr. Z. Geophys.*, **31,** 315–321.

Ahrens, T. J., Lower, J. H., & Lagus, P. L., 1971. Equation of state of forsterite, *J. geophys. Res.*, **76,** 518–528.

Anderson, D. L., 1969. Bulk modulus systematics, *J. geophys. Res.*, **74,** 3857–3864.

Anderson, O. L. & Nafe, J. E., 1965. The bulk modulus-volume relationship for oxide compounds and related geophysical problems, *J. geophys. Res.*, **70,** 3951–3963.

Anderson, O. L., Schreiber, E., Liebermann, R. C. & Soga, N., 1968. Some elastic constant data on minerals relevant to geophysics, *Rev. Geophys.*, **6,** 491–524.

Archambeau, C. B., Flinn, E. A. & Lambert, D. G., 1969. Fine structure of the upper mantle, *J. geophys. Res.*, **74,** 5825–5865.

Bacon, R. H., 1953. The " best " straight line among the points, *Am. J. Phys.*, **21,** 428–446.

Birch, F., 1952. Elasticity and constitution of the Earth's interior, *J. geophys. Res.*, **57,** 227–286.

Birch, F., 1960. The velocity of compressional waves in rocks to 10 kb, Part 1, *J. geophys. Res.*, **65,** 1083–1102.

Birch, F., 1961a. The velocity of compressional waves in rocks to 10 kb, Part 2, *J. geophys. Res.*, **66,** 2199–2224.

Birch, F., 1961b. Composition of the Earth's mantle, *Geophys. J. R. astr. Soc.*, **4,** 295–311.

Birch, F., 1969. Density and composition of the upper mantle: First approximation as an olivine layer, in *The Earth's Crust and Upper Mantle*, edited by P. J. Hart. Geophysical Monograph No. 13, American Geophysical Union, Washington, D.C.

Brace, W. F., 1965. Some new measurements of linear compressibility of rocks, *J. geophys. Res.*, **70,** 391–398.

Brace, W. F., Scholz, C. H. & LaMori, P. N., 1969. Isothermal compressibility of kyanite, andalusite, and sillimanite from synthetic aggregates, *J. geophys. Res.*, **74,** 2089–2098.

Bridgman, P. W., 1948. Rough compression of 177 substances to 40,000 kg/cm^3, *Proc. Am. Acad. Arts Sci.*, **76,** 71–87.

Chung, D. H., 1968. The elastic constants of a cubic crystal subjected to moderately high hydrostatic pressure, *J. Phys. Chem. Solids*, **29,** 417–422.

Chung, D. H., 1970. Effects of iron/magnesium ratio on *P*- and *S*-wave velocities in olivine, *J. geophys. Res.*, **75,** 7353–7361.

Chung, D. H., 1971a. Pressure coefficients of elastic constants for porous materials: Correction for porosity and discussion of literature data, *Earth Planet. Sci. Letters*, **10,** 316–324.

Chung, D. H., 1971b. Equations of state of olivine-transformed spinels in the Mg_2SiO_4-Fe_2SiO_4 system, submitted to *Earth Planet. Sci. Letters.*

Chung, D. H., Wang, H. & Simmons, G., 1970. On the calculation of the seismic parameter ϕ at high pressure and high temperatures, *J. geophys. Res.*, **75,** 5113–5120.

Christensen, N. I., 1966a. Shear wave velocities in metamorphic rocks at pressures to 10 kbar, *J. geophys. Res.*, **70,** 3549–3556.

Christensen, N. I., 1966b. Elasticity of ultrabasic rocks, *J. geophys. Res.*, **71,** 5921–5931.

Christensen, N. I., 1968. Chemical changes associated with the upper mantle structure, *Tectonophysics*, **6,** 331–342.

Dow Chemical Company, 1960. *JANAF Thermochemical Data*, Midland, Michigan.

Fujisawa, H., 1970. Elastic properties of polycrystalline olivine, *Trans, A.G.U.*, **51,** 418. (Abstract only).

Graham, E. K., 1970. Elasticity and composition of the upper mantle, *Geophys. J. R. astr. Soc.*, **20,** 285–302.

Graham, E. K. & Barsch, G. R., 1969. Elastic constants of single-crystal forsterite as a function of temperature and pressure, *J. geophys. Res.*, **74,** 5949–5960.

Kanamori, H., 1970. Velocity and Q of mantle waves, *Phys. Earth Planet. Int.*, **2,** 259–266.

Kanamori, H. & Mizutani, H., 1965. Ultrasonic measurement of elastic constants of rocks under high pressures, *Bull. Earthquake Res. Inst. (Tokyo)*, **43,** 173–194.

Knopoff, L., 1967. Density-velocity relations for rocks, *Geophys. J. R. astr. Soc.*, **13,** 1–8.

Kumazawa, M. & Anderson, O. L., 1969. Elastic moduli, pressure derivatives, and temperature derivatives of single-crystal olivine and single-crystal forsterite, *J. geophys. Res.*, **74,** 5961–5972.

Lazarus, D., 1949. The variation of tha adiabatic elastic constants of KCl, NaCl, CuZn, Cu, and Al with pressure to 10,000 bars, *Phys. Rev.*, **76,** 545–551.

Liebermann, R. C., 1970. Velocity-density systematics for the olivine and spinel phases of Mg_2SiO_4-Fe_2SiO_4, *J. geophys. Res.*, **75,** 4029–4034.

Macdonald, J. R., 1969. Review of some experimental and analytical equations of state, *Rev. mod. Phys.*, **41,** 316–349.

Mao, N., Ito, J., Hays, J. F., Drake, J. & Birch, F., 1970. Composition and elastic constants of hortonolite dunite, *J. geophys. Res.*, **75,** 4071–4076.

Mao, H., Takahashi, T., Bassett, W. A., Weaver, J. S. & Akimoto, S., 1969. Effect of pressure and temperature on the molar volumes of wüstite and three (Fe, $Mg)_2SiO_4$ spinel solid solutions, *J. geophys. Res.*, **74,** 1061–1069.

McQueen, R. G., Marsh, S. P. & Fritz, J. N., 1969. Hugoniot equation of state of 12 rocks, *J. geophys. Res.*, **72,** 4999–5036.

Mizutani, H., Hamano, Y., Ida, Y. & Akimoto, S., 1970. Compressional wave velocities in fayalite, Fe_2SiO_4-spinel, and coesite, *J. geophys. Res.*, **75,** 2741–2747.

Murnaghan, F. D., 1944. Compressibility of media under extreme pressure, *Proc. Nat. Acad. Sci. U.S.*, **30,** 244–246.

Murnaghan, F. D., 1951. *Finite deformation of an elastic solid*, John Wiley & Sons, Inc., New York.

Olinger, B. & Duba, A., 1971. Compression of olivines to 100 kbars, *J. geophys. Res.*, *Res.*, **76,** 2610–2616.

Press, F., 1968. Earth models obtained by Monte Carlo inversion, *J. geophys. Res.*, **73,** 5223–5234.

Press, F., 1969. The suboceanic mantle, *Science*, **165,** 174–176.

Press, F., 1970a. Earth models consistent with geophysical data, *Phys. Earth Planet. Int.*, **3,** 3–22.

Press, F., 1970b. Regionalized earth models, *J. geophys. Res.*, **75,** 6575–6581.

Ringwood, A. E., 1970. Phase transformation and the constitutions of the mantle, *Phys. Earth Planet. Int.*, **3,** 89–155.

Robie, R. A. & Waldbaum, D. R., 1968. Thermodynamic properties of minerals and related substances at 298·15° K and one atmosphere pressure and high temperatures, *Geol. Survey Bull.* **1259,** 256.

Schreiber, E., 1969. The effect of solid solutions upon the bulk modulus and its pressure derivative: Implications for equations of state, *Earth Planet. Sci. Lett.*, **7,** 137–140.

Schreiber, E. & Anderson, O. L., 1967. Pressure derivatives of the sound velocities of polycrystalline forsterite with 6 per cent porosity, *J. geophys. Res.*, **72,** 762–764, and correction p. 3751.

Simmons, G., 1964. Velocity of shear waves in rocks to 10 kb, Part 1, *J. geophys. Res.*, **69,** 1123–1130.

Singh, H. P. & Simmons, G., 1971. Variation of cell parameters of olivines with temperature, to be published.

Skinner, B. J., 1966. Thermal expansion, in *Handbook of Physical Constants, Momoir* **97,** edited by S. P. Clark, Jr., Geological Soc. of America, New York. p. 92.

Soga, N. & Anderson, O. L., 1967. High temperature elasticity and expansivity of forsterite and steatite, *J. Am. Ceram. Soc.*, **50,** 239–242.

Takahashi, T., 1970. Isothermal compression of fayalite at room temperature, *Trans. A.G.U.*, **51,** 827. (Abstract only).

Verma, R. K., 1960. Elasticity of some high-density crystals, *J. geophys. Res.*, **65,** 757–766.

Walsh, J. B., 1965. The effect of cracks on the compressibility of rocks, *J. geophys. Res.*, **70,** 381–390.

Walsh, J. B. & Brace, W. F., 1966. Elasticity of rocks: A review of some recent theoretical studies, *Rock Mechanics & Engineering Geology*, Springer-Verlag, Wien. pp. 284–297.

Whitcomb, D. L., 1970. Reflection of P′P′ seismic waves from discontinuities in the mantle, *J. geophys. Res.*, **75,** 5713–5728.

Appendix

The thermal properties of olivine may be found in a large number of the original literature. Table 8 lists those literature data on thermal expansion α_v and specific heat C_p used in the present work. The α_v values were obtained from Skinner (1966) and Singh & Simmons (1971). The C_p data were based on work of Robie & Waldbaum (1968) and JANAF Thermochemical Data tables (Dow Chemical Company (1960)). Incorporating the elasticity data with these thermal data, Gruneisen's parameters γ_G and δ_s have been evaluated as a function of temperature; results on two temperatures (one at ambient temperature and the other at the Debye temperature) for three chosen olivine compositions are entered in Table 8. The γ_G and δ_s values evaluated at the Debye temperature θ_D represent constant values at high temperature. Values of the Debye temperature of olivine, as listed in the last row of Table 2, were calculated from the present elastic constant data at 296° K in the usual way. The critical thermal gradients for density and P and S wave velocities of 100 Fo, 50 Fo, and 100 Fa olivines are presented in Table 8. In geophysics, the critical thermal gradient for density evaluated at the Debye temperature is of more interest than that evaluated at the ambient temperature.

Table 8

Thermal properties, Grüneisen's parameters, and critical thermal gradients of olivine

Olivine property	Unit	T, °K	Olivine composition, mole % 100 Fo	50 Fo	100 Fa
ρ_0	g cm^{-3}	296	3·217	3·800	4·393
		θ_D†	3·162	3·760	4·364
α_v	10^{-5}/°K	296	2·54	2·45	2·40
		θ_D	3·86	3·20	2·88
C_p	cal/mole−°K	296	28·2	(30·0)‡	31·8
		θ_D	39·2	(39·1)	39·0
$\frac{d \ln K_s}{dT}$	10^{-4}/°K	296	−1·02	−1·07	−1·13
		θ_D	−1·44	−1·39	−1·31
γ_G	None	296	1·21	1·10	1·02
		θ_D	1·26	1·08	0·98
δ_s	None	296	4·0	4·4	4·7
		θ_D	3·7	4·3	4·5
$(\partial T/\partial p)_{V_p}$	°K/kb	296	24	24	23
$(\partial T/\partial p)_{V_s}$	°K/kb	296	12	8	2
$(\partial T/\partial p)_\rho$	°K/kb	296	31	33	35
		θ_D	22	27	30

† The Debye temperature values used here are tabulated in Table 2. They are respectively 754°K for 100 Fo, 633°K for 50 Fo, and 523°K for 100 Fa, and these values were calculated from the present elastic constants data in the usual way.

‡ These values are calculated from the Debye temperature of this material.